Molecular Cancer Therapeutics

A New Class of Antibody–Drug Conjugates with Potent DNA Alkylating Activity

Michael L. Miller, Nathan E. Fishkin, Wei Li, Kathleen R. Whiteman, Yelena Kovtun, Emily E. Reid, Katie E. Archer, Erin K. Maloney, Charlene A. Audette, Michele F. Mayo, Alan Wilhelm, Holly A. Modafferi, Rajeeva Singh, Jan Pinkas, Victor Goldmacher, John M. Lambert, and Ravi V.J. Chari

Abstract

The promise of tumor-selective delivery of cytotoxic agents in the form of antibody–drug conjugates (ADC) has now been realized, evidenced by the approval of two ADCs, both of which incorporate highly cytotoxic tubulin-interacting agents, for cancer therapy. An ongoing challenge remains in identifying potent agents with alternative mechanisms of cell killing that can provide ADCs with high therapeutic indices and favorable tolerability. Here, we describe the development of a new class of potent DNA alkylating agents that meets these objectives. Through chemical design, we changed the mechanism of action of our novel DNA cross-linking agent to a monofunctional DNA alkylator. This modification, coupled with linker optimization, generated ADCs that were well tolerated in mice and demonstrated robust antitumor activity in multiple tumor models at doses 1.5% to 3.5% of maximally tolerated levels. These properties underscore the considerable potential of these purpose-created, unique DNA-interacting conjugates for broadening the clinical application of ADC technology. *Mol Cancer Ther; 15(8); 1870–8. ©2016 AACR.*

Introduction

The limited clinical efficacy of anticancer drugs can be attributed, at least in part, to their inability to kill a sufficient number of cancer cells without causing toxicity. For example, it has been estimated that more than 99% of the cells within a tumor have to be killed to achieve a complete remission in the patient and significantly more to accomplish tumor eradication (1). To improve the effectiveness of cancer chemotherapy, medicinal chemists have developed, through total synthesis or natural product screening, novel compounds that are 1,000-fold more cytotoxic than clinically used anticancer drugs. Accordingly, highly potent tubulin inhibitors, such as maytansine, dolastatin 10 and cryptophycin 52, and DNA-interacting agents, such as adozelesin and bizelesin, were evaluated in the clinic (2–6). However, despite promising antitumor activity *in vivo*, results from clinical studies in cancer patients were disappointing. A common theme emerged that these agents were associated with excessive systemic toxicity and poor antitumor activity, presumably because of their high potency but low tumor selectivity. Tumor-selective delivery through linkage of the cytotoxic agent to monoclonal antibodies directed toward tumor-associated antigens affords a means of lowering the nonspecific toxicity of highly potent drugs, while improving their antitumor activity (7–11). This antibody–drug conjugate (ADC) technology has been validated following the FDA approval of: (i) brentuximab vedotin, a conjugate of an anti-CD30 antibody with the dolastatin derivative, monomethyl auristatin E (12) and (ii) ado-trastuzumab emtansine (T-DM1), a conjugate of trastuzumab with the potent maytansinoid DM1 (13, 14). The realization that ADCs offer a means of reviving compounds that were on their own too toxic to be clinically useful has resulted in burgeoning interest in medicinal chemistry efforts to identify suitable "payloads" for use in ADCs. A majority of ADCs currently in clinical evaluation use highly cytotoxic microtubule-targeted compounds, maytansinoids or dolastatin derivatives, as the payload. To broaden the reach of ADCs to tumors that are clinically insensitive to tubulin agents, there is considerable interest in developing potent cytotoxic agents with alternative mechanisms of cell killing for use as ADC payloads.

Cytotoxic agents that target DNA are widely used in cancer therapy, making them an attractive class for use in ADCs. However, identification of a suitable agent that meets the requirements for use as an effector molecule in ADCs, such as high *in vitro* potency, adequate water solubility, good stability in aqueous solutions, and achievement of a high therapeutic index remains a challenge. For example, ADCs carrying the potent DNA interacting agent calicheamicin are tolerated by humans only at very low doses and one such ADC, gemtuzumab ozogamicin, was withdrawn from the market due to a narrow therapeutic index and related safety concerns (15). ADCs of pyrrolobenzodiazepine (PBD) dimers, potent DNA cross-linkers, have recently been advanced into clinical evaluation (16–18). These ADCs incorporate derivatives of the PBD dimer SJG-136, a highly toxic small molecule with a maximally tolerated dose (MTD) of ~1.2 μg/kg in humans (19).

ImmunoGen, Inc., Waltham, Massachusetts.

Note: Supplementary data for this article are available at Molecular Cancer Therapeutics Online (http://mct.aacrjournals.org/).

Current address for M.F Mayo: Astrazeneca Pharmaceuticals, Waltham, Massachusetts.

Corresponding Author: Ravi V.J. Chari, Department of Chemistry & Biochemistry, ImmunoGen, Inc., 830 Winter Street, Waltham, Massachusetts. Phone: 781-895-0692; Fax: 791-895-0614; E-mail: ravi.chari@immunogen.com

doi: 10.1158/1535-7163.MCT-16-0184

Here we describe the development of a new class of DNA alkylating agents, indolinobenzodiazepine pseudodimers (termed IGNs), which possess a single reactive imine group designed to provide DNA-interacting effector molecules which meet our criteria for use in ADCs. Accordingly, ADCs of these potent DNA alkylators, generated through innovative payload and linker design, are characterized by favorable *in vivo* tolerability and impressive therapeutic indices. Overall, the findings of this study hold considerable promise for improving the success of the ADC technology and providing better therapeutic outcomes for personalized cancer treatments.

Materials and Methods

Cell lines, antibodies, and reagents

The human cancer cell lines KB (epidermoid carcinoma), HSC-2 (squamous cell carcinoma), COLO 205 and LoVo (colorectal adenocarcinoma), RPMI-8226 (myeloma), IGROV-1 (ovarian adenocarcinoma), HL-60 and HEL92.1.7 (leukemia), BJAB (B-cell leukemia), and Namalwa (Burkitt lymphoma) were obtained from ATCC. NB4 and EOL-1 cells were obtained from DSMZ (Germany). The cell lines were purchased within the period of 2000 to 2015; characterized by the vendor; and no further cell line authentication was conducted by the authors. Upon receipt, each line was expanded by passaging 2 to 3 times, aliquoted, and frozen. For use in experiments, cell lines were cultured in media recommended by the vendor in a humidified incubator at 37°C, 5% CO_2 for no longer than 2 months. Humanized anti-folate receptor-α (FRα), anti-EGFR, and anti-CD33 antibodies, chimeric mouse-human anti-EpCAM antibody, and chimeric non-binding control antibody to the Kunitz soybean protease inhibitor (KTI) were all constructed with the human IgG_1 isotype and generated at ImmunoGen, Inc. None of the antibodies used in the studies cross-react with antigen on mouse tissues. The antibody modifying agents SPDB [*N*-succinimidyl 4-(2-pyridyldithio)butanoate] and sulfo-SPDB [*N*-succinimidyl 2-sulfo-4-(2-pyridyldithio) butanoate] were prepared as previously described (20, 21). Additional chemical reagents were purchased from Sigma-Aldrich.

Preparation of IGN ADCs

Full details of the chemical synthesis, including schema, are provided as Supplementary Data. Conjugation of IGN dimers to an antibody was accomplished through two different methods:

ADCs with a noncleavable linkage: The IGN molecules were linked via amide bonds to lysine residues of the antibody. In the IGN molecule bearing an *N*-hydroxysuccinimide (NHS) ester, the imine moiety was reversibly sulfonated by pretreatment with a 5-fold molar excess of sodium bisulfite and then added in an 8-fold molar excess to the antibody in aqueous buffer (50 mmol/L EPPS, pH 8.5), containing 15% *N*,*N*-dimethylacetamide (DMA).

ADCs with a cleavable (disulfide) linkage: The IGN dimer bearing a thiol or an imine-sulfonated thiol was treated *in situ* with SPDB or sulfo-SPDB in DMA, in the presence of a base (*N*-*N*-diisopropylethylamine) to provide the IGN with an activated ester. Addition of the activated IGN in a 6-fold molar excess to the antibody in buffer (50 mmol/L EPPS, pH 8.5) containing 15% DMA resulted in amide bond formation with lysine residues of the antibody.

In both cases, upon completion of conjugation, the reaction mixtures were purified and buffer exchanged into 20 mmol/L histidine, 50 mmol/L sodium chloride, 8.5% w/v sucrose, 0.01% Tween-20, 50 μmol/L sodium bisulfite pH 6.2 formulation buffer using NAP desalting columns (Illustra Sephadex G-25 DNA Grade, GE Healthcare). Dialysis was performed in the same buffer for 4 hours at room temperature and then overnight at 4°C utilizing Slide-a-Lyzer dialysis cassettes (ThermoScientific 30,000 MWCO) to remove any unreacted small molecules. The purified conjugates were found to have an average of 2.5 to 3 IGN molecules linked per antibody (determined by UV-Vis spectroscopy using molar extinction coefficients $\varepsilon_{330\ nm} = 15{,}280\ cm^{-1}(mol/L)^{-1}$ and $\varepsilon_{280\ nm} = 30{,}115\ cm^{-1}(mol/L)^{-1}$ for IGN, and $\varepsilon_{280\ nm} = 201{,}400\ cm^{-1}(mol/L)^{-1}$ for the antibody). The ADCs were more than 95% monomeric (by size exclusion chromatography) and contained <0.1% unconjugated IGN [by acetone precipitation, reverse-phase high-performance (HPLC) analysis].

IGN/DNA adduct formation in cells

EOL-1 cells (8×10^7) were treated with 3 μmol/L diimine IGN or monoimine IGN for 5 hours and 20 hours at 37°C in RPMI media. Cells were then pelleted, washed with PBS, and lysed in TRIS buffer (10 mmol/L, pH 8.5 containing 5 mmol/L EDTA, 0.2% SDS, 200 mmol/L NaCl, 0.1 mg/mL proteinase K) for 5 hours at 37°C. The resulting clear gel was mixed with one volume isopropanol to precipitate gDNA. DNA was pelleted by centrifugation (10,000 rpm, 3 minutes), washed 3 times with isopropanol, and resuspended in 50 mmol/L TRIS, 10 mmol/L EDTA, pH 8 for UV-VIS analysis. DNA was quantified using absorbance measurements. Changes in unadducted DNA after heating at 90°C were determined by measuring the change in absorbance at different wavelengths.

In vitro cytotoxicity

Cytotoxic potencies were assessed using a WST-based cell viability assay as previously described (22). Briefly, human tumor cells (1,000–5,000 cells/well) in serum-containing media were incubated with conjugates ±1 μmol/L of the corresponding unconjugated antibody for 5 days, at 37°C. Cell viability was determined by background corrected WST-8 (Dojindo) absorbance.

Bystander cell killing assay

FRα-positive (transfected) 300.19-FR1#14 (1,000 cells/well) and FRα-negative 300.19-Parental (2,000 cells/well) were treated with ADCs separately, or as a mixed cell population where the number of antigen-positive cells was varied. After 4 days at 37°C, cell viability was measured by addition of Cell Titer Glow (Promega) reagent followed by luminescence measurement.

In vivo antitumor and tolerability experiments

Female CB.17 SCID mice at 6 weeks of age were received from Charles River Laboratories. All *in vivo* procedures were performed in strict accordance with the NIH Guide for the Care and Use of Laboratory Animals. KB, HSC-2, or HL-60 tumor cells (1×10^7) were subcutaneously implanted into mice. Animals bearing established tumors (~100 mm^3; typically 7 days postinoculation) were randomized into treatment groups of 6. Mice received a single intravenous administration of vehicle (0.2 ml/mouse) or IGN ADC on day 1 (i.e., day 8 after tumor cell inoculation). Tumor volumes (V) were calculated by caliper measurements in three dimensions using the formula $V = \text{length} \times \text{width} \times \text{height} \times {}^1/_2$. Tumor size was measured 2 to 3 times weekly and tumor growth

inhibition (T/C value) was determined using the following formula: T/C (%) = Median tumor volume of the treated/Median tumor volume of the control × 100.

With respect to tolerability, all toxicity, changes in body weight, and determination of MTD studies were conducted in non–tumor-bearing CD-1 mice (Charles River Laboratories), using either a weekly × 3 or a single intravenous administration of the ADC.

Results

Preclinical evaluation of ADCs with novel DNA cross-linking activity

IGNs represent a new chemical class of cytotoxic molecules with high *in vitro* potency (IC_{50} values in the low pmol/L range) toward cancer cells. Similar to the PBD dimer SJG-136 (23), the IGN compounds bind to the minor groove of DNA followed by covalent reaction of guanine residues with the two imine functionalities in the molecule resulting in cross-linking of DNA. Substitution of the pyrrolo group of the PBD molecule with an indolino moiety conferred ∼10-fold higher potency *in vitro* as compared with SJG-136, possibly due to faster rate of adduct formation with DNA (Supplementary Fig. S1, Supplementary Table S1). In addition, incorporation of a phenyl group between the two monomer units provides a site for linker attachment. ADCs were prepared with three monoclonal antibodies that target cell surface antigens EpCAM, CD33, and FRα (Fig. 1A). In these ADCs, the IGN molecules were linked through amide bonds to lysine residues on the antibody, with approximately 3 IGN molecules per antibody. The ADCs displayed high, antigen-specific cytotoxicity *in vitro*. For example, the anti-EpCAM-IGN ADC **1a** was effective in killing the multidrug-resistant (MDR) human colon tumor cell line HCT-15, with an IC_{50} value of 6 pmol/L. The addition of an excess (1 μmol/L) of unconjugated antibody abrogated the cytotoxic effect demonstrating antigen-specific killing (Supplementary Fig. S2A). The anti-CD33-IGN ADC **1b** killed the leukemia cell line NB4, with an IC_{50} value of 3 pmol/L, despite the low antigen expression on these cells (∼7,000 CD33 molecules/cell). Antigen-negative Namalwa cells were >100-fold less sensitive, again demonstrating antigen-dependent cytotoxicity (Supplementary Fig. S2B). In an efficacy study in SCID mice bearing human tumor xenografts established subcutaneously with the human epidermoid carcinoma cell line KB, the anti-FRα ADC **1c** displayed dose-dependent antitumor activity starting at a single intravenous dose as low as ∼0.5 mg/kg conjugate (10 μg/kg conjugated IGN; Fig. 1B). However, during the evaluation of the MTD in non–tumor-bearing CD-1 mice, a troubling toxicity pattern emerged, as mice that had been treated with the ADC (3.75 mg/kg, qw × 3) displayed prolonged loss in body weight, including delayed lethality of some of the animals (Fig. 1C).

Changing the IGN mechanism of action

The undesired prolonged toxicity profile of the first IGN ADC tested in mice led us to investigate whether the DNA cross-linking feature of the IGN dimer, through its diimine functionality, was leading to an inability of the animals to thrive. To explore other structural designs, we had to first determine the contribution of the cross-linking mechanism to *in vitro* potency. Controlled reduction of the IGN diimine **1** using sodium borohydride

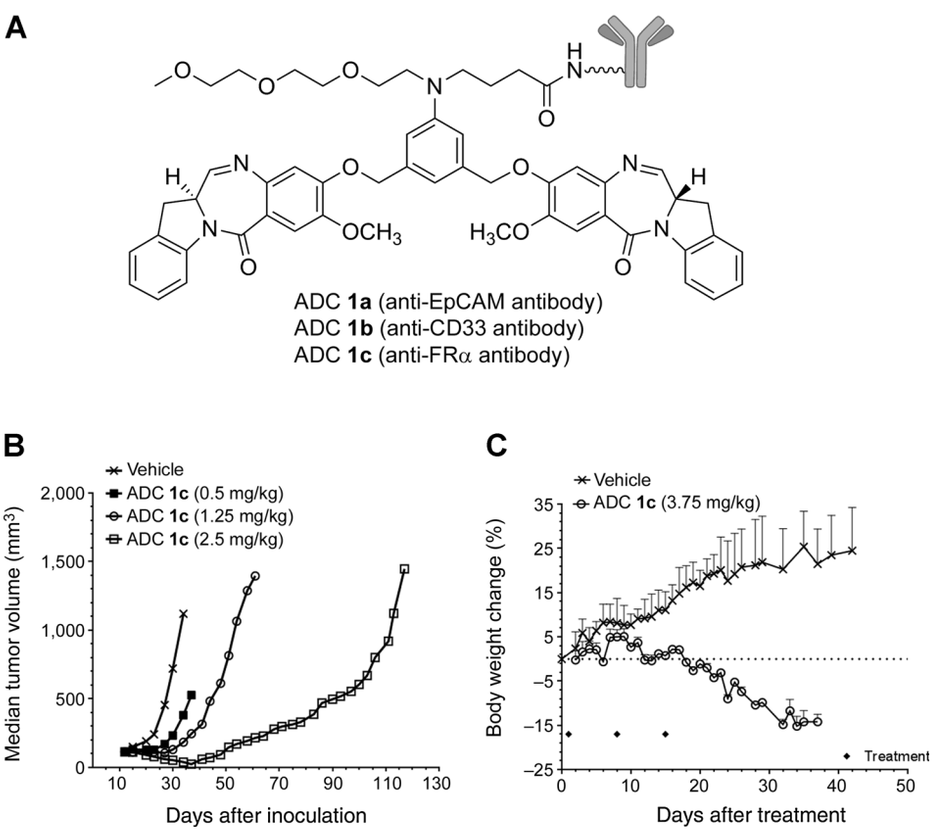

Figure 1.
In vivo antitumor activity and tolerability of ADCs with DNA cross-linking (diimine) IGN. **A,** structural representation of the diimine IGN ADCs 1a (anti-EpCAM), 1b (anti-CD33), and 1c (anti-FRα) in which the IGN is linked via a noncleavable amide bond. **B,** dose-dependent antitumor activity of anti-FRα ADC 1c (single i.v. injection, 0.5–2.5 mg/kg) in a subcutaneous xenograft model established with the human epidermoid carcinoma cell line KB in SCID mice. **C,** changes in body weight over time in non–tumor-bearing CD-1 mice treated with 3 i.v. injections (day 1, 8, 15; circles) of the anti-FRα ADC 1c (3.75 mg/kg) compared with vehicle-treated mice on the same schedule. In the treatment arm, deaths occurred in 2 of 4 animals.

provided the partially reduced monoimine compound **3**, which can bind to and alkylate DNA but cannot cross-link. Complete reduction gave the fully reduced diamine version **2** that can only bind to DNA but not react with it (Fig. 2). The cytotoxicity of these unconjugated IGN compounds was evaluated *in vitro*. As expected, the diimine cross-linker **1** was highly potent, with IC_{50} values ranging from 1 to 11 pmol/L. Surprisingly, the monoimine DNA alkylator version **3** was only about 2- to 4-fold less potent toward a panel of 9 cancer cell lines [encompassing both solid tumor and leukemia/lymphoma cell lines, including the MDR-positive cell line HEL92.1.7 (ref. 24)], while the fully reduced diamine molecule **2**, which can still bind to DNA, but is incapable of alkylation, was 5- to 30-fold less cytotoxic than **1** (Supplementary Table S2).

To understand whether there were any differences in the interaction of the monoimine and diimine forms of IGN (Supplementary Fig. S3A) with DNA, we incubated the human acute myeloid leukemia (AML) cell line EOL-1 with each of the compounds and quantified total DNA and IGN-adducted DNA (Supplementary Table S3). While the two compounds co-purify with cellular DNA to a comparable final extent after 20 hours, the monoimine-containing IGN achieves only half the level of DNA modification as that achieved with the diimine at the earlier 5-hour time point (39 ± 2 vs. 75 ± 3 pmol adduct/μg DNA, respectively). This finding suggests that although both monoimine and diimine forms of IGN produce adducts with cellular DNA, they interact with DNA at different rates. The resulting IGN–DNA adducts isolated from treated EOL-1 cells were subsequently heated at 90°C, and the rate of reversal of the adduct was determined by LC-MS. Thermal reversibility of the DNA adduct of the diimine was about 2.5-fold slower than that of the DNA adduct of the monoimine (Supplementary Fig. S3B), suggesting that the diimine compound forms a relatively more stable adduct to cellular DNA than the monoimine analogue. The IGN monoimine and diimine also interacted differently with acellular DNA in a comet assay, with the monoalkylator forming extensive tails, whereas the cross-linker gave markedly shorter tails, indicative of DNA cross-linking (Supplementary Fig. S3C).

The *in vitro* potency of ADCs of the diimine and monoimine forms was compared using three antibodies against different antigen targets. The ADCs (**3a-c**, Fig. 3A) of the monoimine form of IGN were all highly cytotoxic, with IC_{50} values ranging from 2 to 60 pmol/L, and in general were only between 1.3- and 6-fold less potent than the corresponding ADCs (**1a-c**) of the cross-linker form (Table 1). The anti-CD33 ADC **3b** of the monoimine form of IGN efficiently killed the MDR-positive cell line HEL92.1.7 with an IC_{50} of 30 pmol/L and was only about 4-fold less cytotoxic than ADC **1b** with the cross-linking form. *In vivo*, the anti-FRα ADC **3c** displayed dose-dependent antitumor activity similar to that noted with the ADC **1c** of the cross-linker in the KB model, albeit the doses were 2-fold higher (Fig. 3B). In contrast to mice that had been treated with ADC of the cross-linker (Fig. 1C), body weights in non–tumor-bearing CD-1 mice treated with monoimine IGN ADC, using the same antibody and schedule as **1c** but at a two-fold higher dose (7.5 mg/kg, qw × 3), tracked with that of the vehicle control, with no evidence of prolonged or delayed

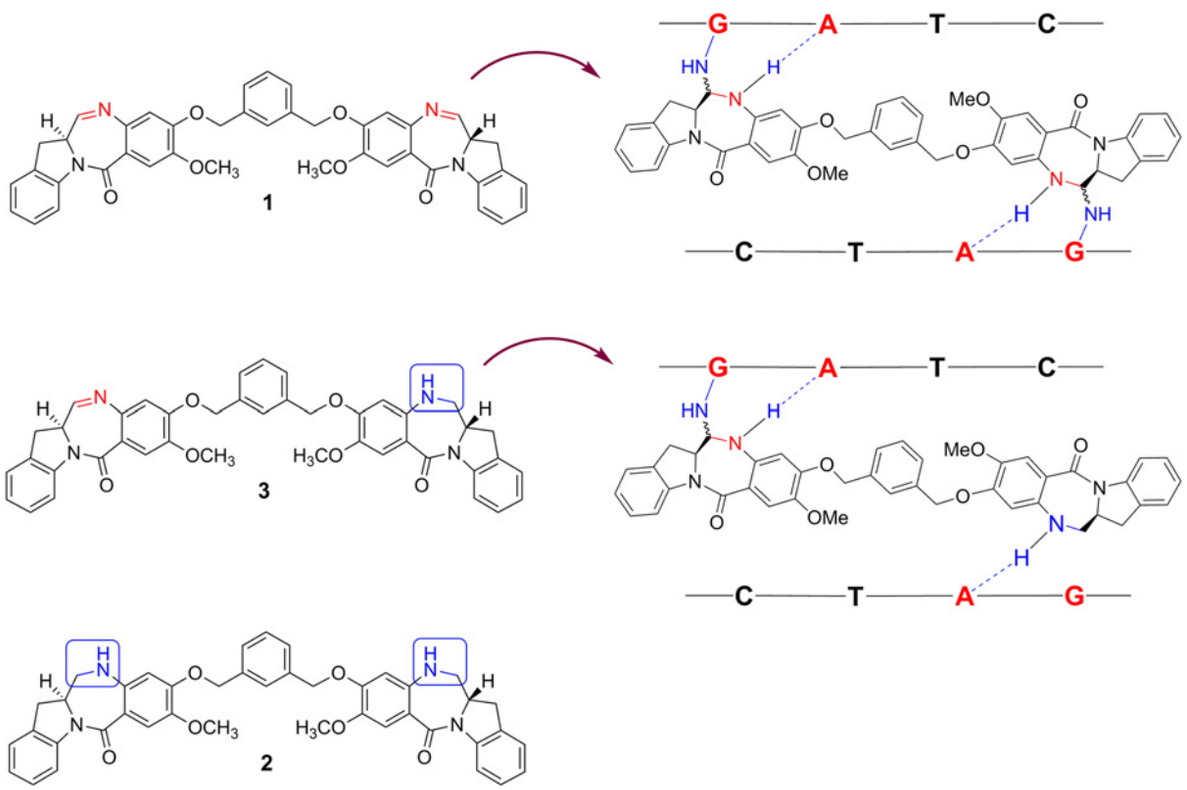

Figure 2.
Structures of IGNs with different states of imine reduction (unreduced, partially, fully reduced) and pictorial representation of their interaction with DNA.

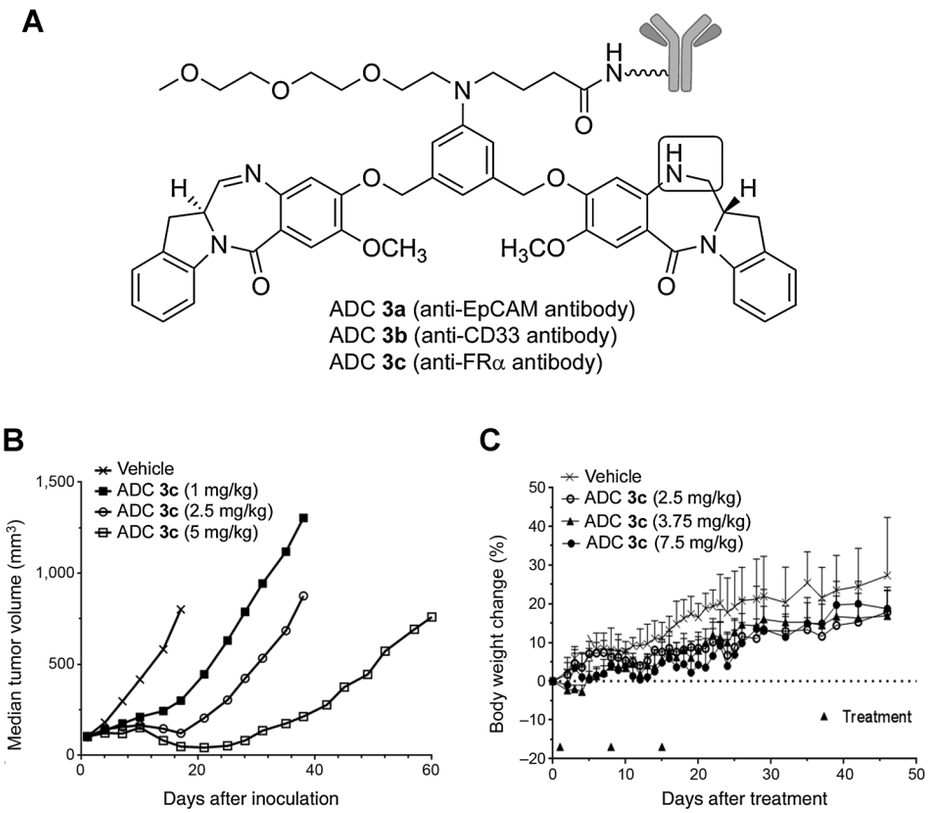

Figure 3.
A, structures of the monoimine IGN ADCs 3a (anti-EpCAM), 3b (anti-CD33), and 3c (anti-FRα). **B,** dose-dependent antitumor activity of the anti-FRα ADC 3c (single i.v. injection, 1, 2.5, and 5 mg/kg) in KB xenografts. **C,** body weight changes in non–tumor-bearing CD-1 mice treated with 3 intravenous injections (day 1, 8, 15; arrowheads) of ADC 3c (2.5, 3.75, and 7.5 mg/kg).

toxicity (Fig. 3C). These results suggest that the DNA cross-linking feature of the IGN compound used in **1c** was the primary cause of prolonged toxicity. The MTD of the ADC **3c** in non–tumor-bearing CD-1 mice, dosed as a single injection, was estimated to be 10 mg/kg conjugate (200 μg/kg linked IGN). The minimum effective dose (MED), determined as previously described (25), in the *in vivo* efficacy model (Fig. 3B) was estimated to be about 1 mg/kg (20 μg/kg linked IGN) giving an *in vivo* therapeutic index (TI), defined as the ratio of MTD to MED, of about 10.

Linker selection

In the ADCs **3a-c** the IGN molecule is attached to the antibody via a noncleavable linker that relies on lysosomal degradation of the antibody to release the lysine-linked IGN molecule, in a manner analogous to the ADC T-DM1 (26). We designed an IGN compound which retained the short tri-oxyethylene spacer found in the IGN structures in ADCs **3a-c** but incorporated a sterically hindered thiol substituent to enable conjugation to antibodies via disulfide linkers that can be cleaved inside the cell to release the active cytotoxic molecule. The anti-FRα ADC **4a** (Fig. 4A), bearing the IGN molecule 4 (DGN462) linked via a disulfide bond, displayed high antigen-specific cytotoxicity *in vitro* with an IC_{50} value of 12 pmol/L (Supplementary Fig. S4). The killing effect was diminished about 60-fold by the addition of an excess of unconjugated antibody, demonstrating the immunologic specificity of the conjugate. ADC **4a** was considerably more active *in vivo* than **3c**. When tested in mice bearing established subcutaneous KB xenografts, dose-dependent antitumor activity was observed (Fig. 4B). Treatment with a single intravenous injection at 2.3 mg/kg ADC **4a** (40 μg/kg linked IGN) resulted in significant tumor growth delay, while higher doses (4.6 and 6.9 mg/kg) produced complete tumor regression lasting more than 60 days (duration of the experiment). Importantly, the MTD of this ADC in non–tumor-bearing CD-1 mice was approximately 35 mg/kg ADC (700 μg/kg linked IGN) and thus considerably less toxic than the ADC with the noncleavable linker **3c**. The higher MTD coupled with the improved antitumor activity (MED ∼1 mg/kg or 20 μg/kg linked IGN) resulted in an *in vivo* TI of ∼35 in this model.

Table 1. Comparative *in vitro* cytotoxicity of IGN ADCs with a diimine (**1a-c**) or a monoimine (**3a-c**)

Antibody	Cell line	Antigen expression (×1,000)	IC_{50}, pmol/L 1a-c	3a-c
Anti-EpCAM	COLO 205	1,000	3	8
	LoVo	350	10	60
Anti-CD33	HL-60	20	0.7	2
	HEL92.1.7	39	7	30
	EOL-1	10	2	3
	NB4	7	3	9
Anti-FRα	KB	3,000	15	20

Bystander cell killing

Maytansinoid and auristatin ADCs with cleavable linkers generate intracellular catabolites that can diffuse out of the targeted cells into proximal antigen-negative cells, to induce killing of these "bystander" cells (27, 28). To understand the possible cause of the improved antitumor activity of the IGN ADC with a disulfide linker relative to that observed with the noncleavable linker, we compared the *in vitro* bystander killing activities of the

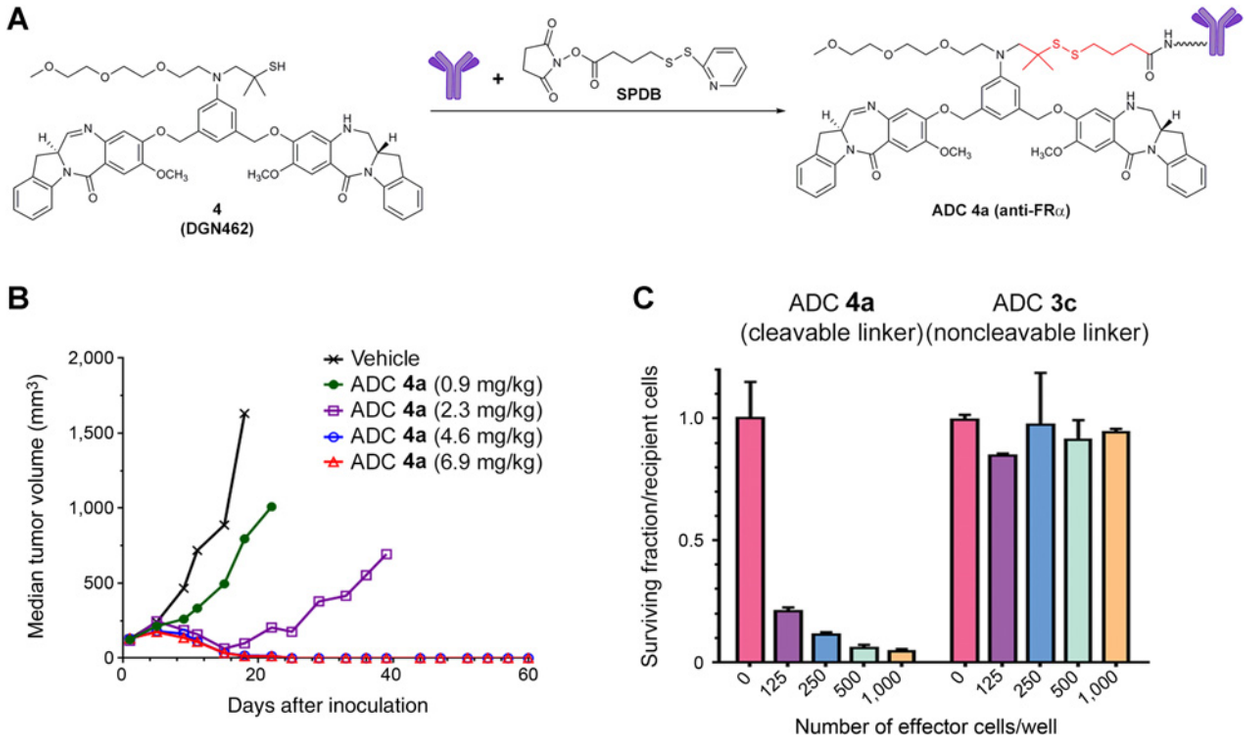

Figure 4.

Improved antitumor and bystander cell killing activity of an alkylator IGN ADC through incorporation of a cleavable linker. **A,** scheme for the preparation of an IGN ADC (anti-FRα ADC 4a) with a disulfide linker. **B,** dose-dependent antitumor activity of ADC 4a with a disulfide linker (single i.v. injection, 0.9–6.9 mg/kg) in a subcutaneous KB xenograft model in SCID mice. **C,** comparison of bystander cell killing activity of the anti-FRα ADC 4a with a cleavable (disulfide) linker versus the corresponding ADC 3c with a noncleavable linker.

two ADCs. In this assay, a fixed number of antigen-negative cells are cocultured with varying number of antigen-positive cells and treated with the ADC. Treatment with ADC **4a**, bearing the cleavable disulfide linker, resulted in augmented killing of proximal antigen-negative cells as the numbers of antigen positive cells in the culture were increased, consistent with the expectation that higher cell number would produce greater amount of catabolite that can diffuse into, and kill, the bystander cells (Fig. 4C). In contrast, ADC **3c** with a noncleavable linker was incapable of killing bystander cells even when a high number of antigen-positive cells were added to the mixed culture.

Linker optimization and *in vivo* antitumor activity

We have previously shown that incorporation of a sulfonate group in the disulfide linker confers improved water solubility to maytansinoid ADCs and also enhances antitumor efficacy *in vivo* (21, 29). By analogy, we incorporated the charged sulfonate group in the IGN ADCs as part of the linker optimization effort. To further improve aqueous solubility of the resulting conjugate, beyond that provided by the charged linker, we sulfonated the imine moiety of the IGN molecule by treatment with sodium bisulfite to provide an optimized ADC (Fig. 5A). The sulfonated compound spontaneously reverses to the free imine *ex vivo* in human plasma, and under cell culture conditions, and thus the sulfonated and unsulfonated compounds are equipotent *in vitro* (Supplementary Fig. S5). We prepared conjugates (**5a-c**) with three different monoclonal antibodies: anti-EGFR that does not inhibit ligand binding or receptor signaling and has no inherent antitumor activity; anti-CD33 targeting the CD33 antigen expressed on the surface of AML cells; and a control antibody (anti-KTI), which does not recognize any cell surface antigen. The two ADCs targeting cell surface antigens and the nonbinding control ADC, with ~2.5 to 3 IGN molecules linked per antibody, were then evaluated for antitumor activity in human tumor xenograft models in SCID mice. In the first model, we compared the efficacy of the anti-EGFR conjugate **5a** with the nonbinding control **5c** in mice bearing HSC-2 human head and neck squamous cell carcinoma xenografts (Fig. 5B). The targeting conjugate was highly active at doses well below the MTD, with even the lowest dose tested (1.3 mg/kg, single intravenous injection) causing complete tumor regression in 5 of 6 animals, with 2 of the 6 mice being tumor-free at day 100 (conclusion of study). Treatment at the two higher doses (2.5 and 5 mg/kg) rendered all of the animals tumor-free at day 100. The antitumor activity was antigen-specific, as the nonbinding control ADC had only marginal activity in this model. In an *in vivo* model established using the human AML cell line HL-60 (Fig. 5C), the anti-CD33 ADC **5b** (termed anti-CD33–sulfonated DGN462) was active at a single intravenous dose of just 0.5 mg/kg (10 μg/kg IGN), giving an *in vivo* therapeutic index of about 70. Treatment at a 3-fold higher dose resulted in complete tumor regression in 6 of 6 animals. Importantly, the mixture of unconjugated antibody and free IGN (DGN462) was inactive at equivalent doses demonstrating the power of antibody-mediated delivery (Fig. 5C).

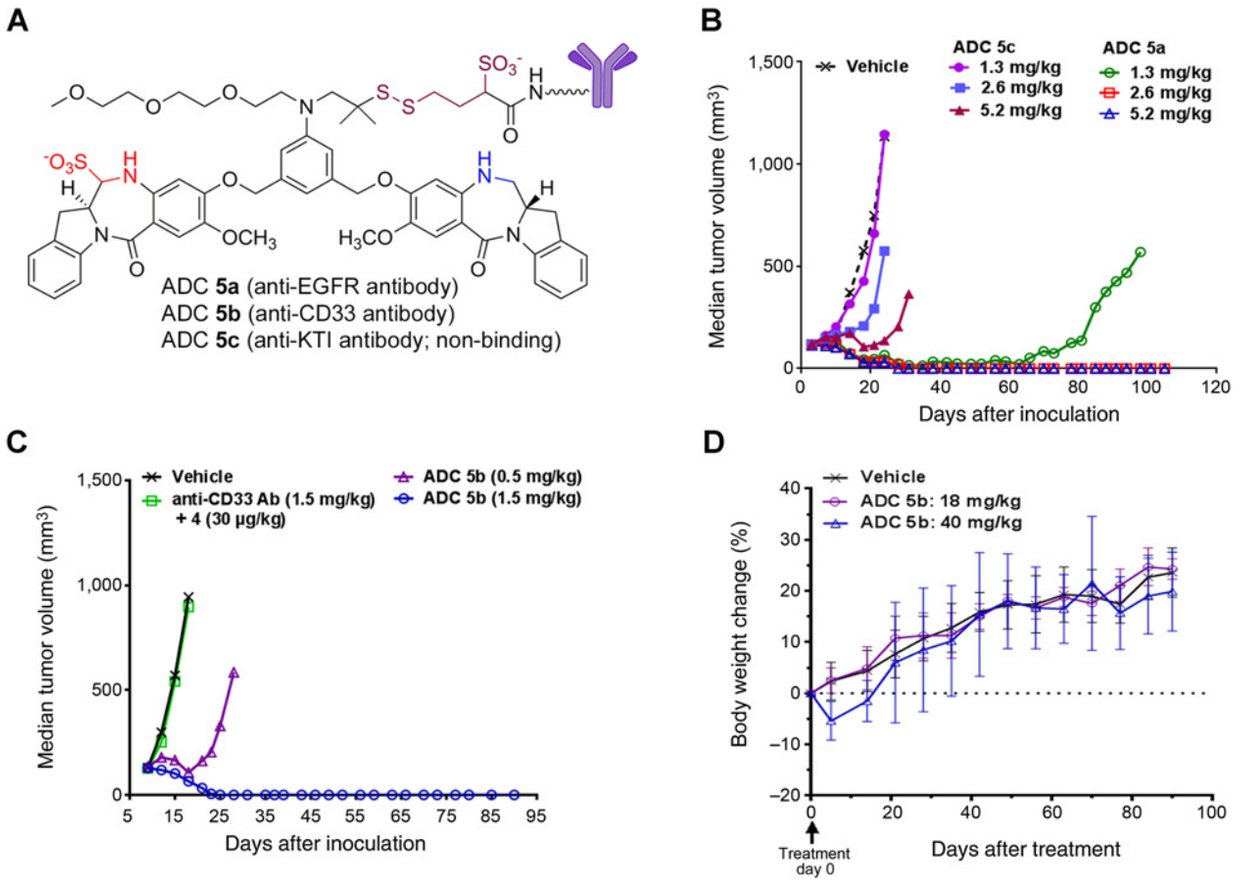

Figure 5.

In vivo antitumor activity and toxicity of ADCs of an IGN alkylator linked to antibodies via an optimized cleavable linker. **A,** structural representation of IGN ADCs 5a-c prepared with a charged linker and reversible imine sulfonation (5a, anti-EGFR; 5b, anti-CD33; 5c, anti- KTI). **B,** *in vivo* antitumor activity of the anti-EGFR ADC 5a in comparison to the nonbinding ADC 5c in head and neck carcinoma HSC-2 xenografts in SCID mice. The anti-EGFR antibody used for ADC conjugation has no inherent antitumor activity. **C,** *in vivo* antitumor activity of the anti-CD33 ADC 5b in comparison to a mixture of unconjugated IGN (4) plus the anti-CD33 antibody at equivalent doses to the ADC in a HL60 xenograft model. **D,** change in body weight in CD-1 mice treated with the ADC 5b compared with the vehicle control.

Tolerability profile of the optimized IGN ADC in mice

The MTD of the ADC **5b**, with the charged disulfide linker, was determined to be 700 μg/kg linked IGN (35 mg/kg conjugate dose) in CD-1 mice after a single intravenous injection, similar to that of ADC prepared with the uncharged disulfide linker. Preliminary evaluation of linker effects on toxicology of the ADCs was performed. Treatment with the imine-sulfonated form of ADC **3b**, with a noncleavable linker, at a dose of 10 mg/kg caused a considerable spike in liver enzymes [17- and 35-fold increase in aspartate aminotransferase (AST) and alanine aminotransferase (ALT), respectively] and an 8-fold decrease in platelet count. In contrast, treatment with the ADC **5b** with the cleavable linker at a 4-fold higher dose (40 mg/kg) caused only mild hematologic toxicity with a small decrease (2- to 4-fold) in platelets, neutrophils, and lymphocytes, and no effects on liver enzyme levels. Animals were observed for 90 days and the body weights of mice treated with 18 and 40 mg/kg doses both tracked with control animals (Fig. 5D).

Discussion

ADCs that contain potent tubulin-interacting compounds, such as the maytansinoids and auristatins, have often displayed a good therapeutic index *in vivo* resulting in the advancement of several into clinical evaluation. However, developing ADCs that meet the criteria for clinical advancement using potent DNA-interacting agents has been a challenge owing to at least two factors: (i) a paucity of DNA-interacting compounds that meet the requirement of high potency, stability, and solubility in aqueous formulation and (ii) difficulty in achieving a sufficient therapeutic index *in vivo* (30). The duocarmycins and CC-1065 analogues are potent DNA minor groove binders and alkylators that are being evaluated in ADCs, yet compounds from these two classes suffer the major drawbacks of low aqueous stability and solubility, in turn making them poorly suited for use in ADCs. Furthermore, while conversion of these compounds to prodrugs has provided an avenue to their ADC use, the relative efficiency of activation of prodrug forms in humans as compared with mice remains unknown. In this regard,

an anti-CD70 ADC of a duocarmycin carbamate prodrug failed to achieve any objective responses in a phase I clinical study (31), whereas an ADC with a new duocarmycin prodrug design has recently entered clinical evaluation (32).

To address these factors, we developed a new class of highly cytotoxic molecules, the IGNs, consisting of indolinobenzodiazepine pseudodimers for use as effector molecules for ADCs. Our first set of ADCs prepared with the "diimine" cross-linking IGN compound were toxic at low doses in mice and further displayed a phenomenon of delayed onset of prolonged body weight loss. Although cross-linking PBD dimers with two imines have advanced to the clinic, the unusual toxicity findings with an ADC bearing the IGN-diimine compound made us pause. For many clinically used anticancer drugs, such as vincristine, cyclophosphamide, and carboplatin, there is a strong correlation between the LD_{10} in mice and the human MTD (33). For example, the LD_{10} values in mice for cyclophosphamide and carboplatin are 340 and 495 mg/m^2 compared with a human MTD of 370 and 440 mg/m^2, respectively. For highly potent molecules, such as dolastatin-10, a tubulin-interacting agent, or adozelesin, a DNA alkylator, the MTD (3, 5) in humans is about 33% of the mouse LD_{10}. In contrast, the highly cytotoxic DNA cross-linking agents, bizelesin (a duocarmycin analog dimer) and SJG-136 (a PBD dimer) are poorly tolerated in humans compared with mice, with only about 3.5% of the mouse LD_{10} achievable in humans (6, 19). On the basis of the delayed toxicity profile and the potential for a low achievable dose in humans, we decided not to advance ADCs of the cross-linking IGN subclass. Controlled reduction of one of the imine moieties of the IGN diimine changed its mechanism of action, by eliminating its ability to cross-link DNA while simultaneously retaining monoalkylation functionality. ADCs of the monoimine compounds maintained high *in vitro* potency, were only about 2- to 4-fold less cytotoxic than the cross-linking form, and displayed pronounced antitumor activity *in vivo*.

Importantly, the ADC of the alkylating monoimine form of IGN, with the same noncleavable linker as that used in the ADC of the IGN diimine, no longer displayed delayed or prolonged toxicity in mice. Linker optimization led to the design of IGN-ADCs with hindered disulfide linkers that provided good bystander killing of proximal cancer cells and thus displayed considerably superior antitumor activity *in vivo*, compared with the ADC with the noncleavable linker. Bystander killing may play an important role clinically in the treatment of solid tumors that often express the antigen in a heterogeneous manner or where all tumor cells may not be accessible to the ADC. Notably, the ADC with the disulfide linker tested here was also better tolerated, with a ~3.5-fold greater MTD in mice than that with the ADC with a noncleavable linker. These results indicate that, in the ADCs described here, the bystander killing feature provides increased antitumor activity but not increased systemic toxicity. Interestingly, this finding is counterintuitive, since ADCs of tubulin-interacting agents, maytansinoids or auristatins, with cleavable linkers (disulfide or peptidase-labile) are reported to be less tolerable in mice, compared with those prepared with noncleavable linkers (34, 35). Further studies on the *in vivo* catabolism and distribution of these ADCs are ongoing and may provide some insight into the cause of the improved tolerability of the ADC with the cleavable linker. Dose-dependent, antigen-specific antitumor activity was demonstrated using ADCs against three different targets. The therapeutic index attained in these models ranged from 28 to 70, fulfilling our original goal of developing an ADC of a DNA-interacting effector molecule with a high therapeutic index for further development. Our first IGN ADC (IMGN779, **5b**) targeting CD33 is now being advanced towards clinical evaluation.

Disclosure of Potential Conflicts of Interest

C.A. Audette has ownership interest (including patents) in shares of stock. V. Goldmacher has ownership interest (including patents) in ImmunoGen, Inc. common stock. J.M. Lambert and R.V.J. Chari have ownership interest (including patents) in ImmunoGen Inc. No potential conflicts of interest were disclosed by the other authors.

Authors' Contributions

Conception and design: M.L. Miller, N.E. Fishkin, W. Li, K.R. Whiteman, M.F. Mayo, J. Pinkas, R.V.J. Chari

Development of methodology: M.L. Miller, N.E. Fishkin, W. Li, K.R. Whiteman, E.E. Reid, K.E. Archer, E.K. Maloney, J. Pinkas, V. Goldmacher, R.V.J. Chari

Acquisition of data (provided animals, acquired and managed patients, provided facilities, etc.): M.L. Miller, W. Li, K.R. Whiteman, E.E. Reid, K.E. Archer, E.K. Maloney, C.A. Audette, M.F. Mayo, A. Wilhelm, H.A. Modafferi

Analysis and interpretation of data (e.g., statistical analysis, biostatistics, computational analysis): M.L. Miller, N.E. Fishkin, W. Li, K.R. Whiteman, Y. Kovtun, E.K. Maloney, C.A. Audette, M.F. Mayo, A. Wilhelm, H.A. Modafferi, V. Goldmacher, R.V.J. Chari

Writing, review, and/or revision of the manuscript: M.L. Miller, N.E. Fishkin, Y. Kovtun, J. Pinkas, V. Goldmacher, J.M. Lambert, R.V.J. Chari

Administrative, technical, or material support (i.e., reporting or organizing data, constructing databases): E.K. Maloney, A. Wilhelm, R. Singh

Study supervision: M.L. Miller, N.E. Fishkin, M.F. Mayo, J. Pinkas, R.V.J. Chari

Other (head of the R & D group guiding the research and Chief Science Officer during the time the research was conducted): J.M. Lambert

Acknowledgments

The authors thank Richard Bates for carefully editing the article and Tom Keating, Carol Hausner, and Richard Gregory for their helpful suggestions. They also thank Barbara Leece, Andre Dandeneau, Gregory Jones, Megan Bogalhas, and Lintao Wang for their contribution to some of the experimental work and Robert Lutz for his inspirational support. They are also grateful to Nicole Dewhurst at Helix3, Inc. for performing the acellular comet assays.

Grant Support

All work was funded by ImmunoGen, Inc.

The costs of publication of this article were defrayed in part by the payment of page charges. This article must therefore be hereby marked *advertisement* in accordance with 18 U.S.C. Section 1734 solely to indicate this fact.

Received March 29, 2016; revised May 9, 2016; accepted May 9, 2016; published OnlineFirst May 23, 2016.

References

1. Frei E III. Combination cancer therapy: presidential address. Cancer Res 1972;32:2593–607.
2. Issell BF, Crooke ST. Maytansine. Cancer Treat Rev 1978;5:199–207.
3. Pitot HC, McElroy EA Jr, Reid JM, Windebank AJ, Sloan JA, Erlichman C, et al. Phase I trial of dolastatin-10 (NSC 376128) in patients with advanced solid tumors. Clin Cancer Res 1999;5:525–31.
4. Edelman MJ, Gandara DR, Hausner P, Israel V, Thornton D, DeSanto J, et al. Phase 2 study of cryptophycin 52 (LY355703) in patients previously treated with platinum based chemotherapy for advanced non-small cell lung cancer. Lung Cancer 2003;39:197–9.
5. Cristofanilli M, Bryan WJ, Miller LL, Chang AY, Gradishar WJ, Kufe DW, et al. Phase II study of adozelesin in untreated metastatic breast cancer. Anticancer Drugs 1998;9:779–82.
6. Pitot HC, Reid JM, Sloan JA, Ames MM, Adjei AA, Rubin J, et al. A Phase I study of bizelesin (NSC 615291) in patients with advanced solid tumors. Clin Cancer Res 2002;8:712–7.

7. Chari RV, Miller ML, Widdison WC. Antibody-drug conjugates: An emerging concept in cancer therapy. Angewandte Chemie 2014;53: 3796–827.
8. Chudasama V, Maruani A, Caddick S. Recent advances in the construction of antibody-drug conjugates. Nat Chem 2016;8:114–9.
9. Diamantis N, Banerji U. Antibody-drug conjugates-an emerging class of cancer treatment. Br J Cancer 2016;114:362–7.
10. Chari RVJ. Targeted cancer therapy: conferring specificity to cytotoxic drugs. Acc Chem Res 2008;41:98–107.
11. Sievers EL, Senter PD. Antibody-drug conjugates in cancer therapy. Annu Rev Med 2013;64:15–29.
12. Katz J, Janik JE, Younes A. Brentuximab Vedotin (SGN-35). Clin Cancer Res 2011;17:6428–36.
13. Amiri-Kordestani L, Blumenthal GM, Xu QC, Zhang L, Tang SW, Ha L, et al. FDA approval: ado-trastuzumab emtansine for the treatment of patients with HER2-positive metastatic breast cancer. Clin Cancer Res 2014;20: 4436–41.
14. Lambert JM, Chari RV. Ado-trastuzumab Emtansine (T-DM1): an antibody-drug conjugate (ADC) for HER2-positive breast cancer. J Med Chem 2014;57:6949–64.
15. Petersdorf SH, Kopecky KJ, Slovak M, Willman C, Nevill T, Brandwein J, et al. A phase 3 study of gemtuzumab ozogamicin during induction and postconsolidation therapy in younger patients with acute myeloid leukemia. Blood 2013;121:4854–60.
16. Saunders LR, Bankovich AJ, Anderson WC, Aujay MA, Bheddah S, Black K, et al. A DLL3-targeted antibody-drug conjugate eradicates high-grade pulmonary neuroendocrine tumor-initiating cells in vivo. Sci Transl Med 2015;7:302ra136.
17. Kung Sutherland MS, Walter RB, Jeffrey SC, Burke PJ, Yu C, Kostner H, et al. SGN-CD33A: a novel CD33-targeting antibody-drug conjugate utilizing a pyrrolobenzodiazepine dimer is active in models of drug-resistant AML. Blood 2013;122:1455–63.
18. Jeffrey SC, Burke PJ, Lyon RP, Meyer DW, Sussman D, Anderson M, et al. A potent anti-CD70 antibody-drug conjugate combining a dimeric pyrrolobenzodiazepine drug with site-specific conjugation technology. Bioconjug Chem 2013;24:1256–63.
19. Hochhauser D, Meyer T, Spanswick VJ, Wu J, Clingen PH, Loadman P, et al. Phase I study of sequence-selective minor groove DNA binding agent SJG-136 in patients with advanced solid tumors. Clin Cancer Res 2009;15: 2140–7.
20. Widdison WC, Wilhelm SD, Cavanagh EE, Whiteman KR, Leece BA, Kovtun Y, et al. Semisynthetic maytansine analogues for the targeted treatment of cancer. J Med Chem 2006;49:4392–408.
21. Zhao RY, Wilhelm SD, Audette C, Jones G, Leece BA, Lazar AC, et al. Synthesis and evaluation of hydrophilic linkers for antibody-maytansinoid conjugates. J Med Chem 2011;54:3606–23.
22. Kovtun YV, Audette CA, Mayo MF, Jones GE, Doherty H, Maloney EK, et al. Antibody-maytansinoid conjugates designed to bypass multidrug resistance. Cancer Res 2010;70:2528–37.
23. Hartley JA, Spanswick VJ, Brooks N, Clingen PH, McHugh PJ, Hochhauser D, et al. SJG-136 (NSC 694501), a novel rationally designed DNA minor groove interstrand cross-linking agent with potent and broad spectrum antitumor activity: part 1: cellular pharmacology, in vitro and initial in vivo antitumor activity. Cancer Res 2004;64:6693–9.
24. Foley KP, Zhou D, Borella C, Wu Y, Zhang M, Jiang J, et al. The vascular disrupting agent STA-9584 exhibits potent antitumor activity by selectively targeting microvasculature at both the center and periphery of tumors. J Pharmacol Exp Ther 2012;343:529–38.
25. Bissery MC, Guenard D, Gueritte-Voegelein F, Lavelle F. Experimental antitumor activity of taxotere (RP 56976, NSC 628503), a taxol analogue. Cancer Res 1991;51:4845–52.
26. Lewis Phillips GD, Li G, Dugger DL, Crocker LM, Parsons KL, Mai E, et al. Targeting HER2-positive breast cancer with trastuzumab-DM1, an antibody-cytotoxic drug conjugate. Cancer Res 2008;68:9280–90.
27. Kovtun YV, Audette CA, Ye Y, Xie H, Ruberti MF, Phinney SJ, et al. Antibody-drug conjugates designed to eradicate tumors with homogeneous and heterogeneous expression of the target antigen. Cancer Res 2006;66:3214–21.
28. Okeley NM, Miyamoto JB, Zhang X, Sanderson RJ, Benjamin DR, Sievers EL, et al. Intracellular activation of SGN-35, a potent anti-CD30 antibody-drug conjugate. Clin Cancer Res 2010;16:888–97.
29. Ab O, Whiteman KR, Bartle LM, Sun X, Singh R, Tavares D, et al. IMGN853, a folate receptor-alpha (FRalpha)-targeting antibody-drug conjugate, exhibits potent targeted antitumor activity against FRalpha-expressing tumors. Mol Cancer Ther 2015;14:1605–13.
30. Zhao RY, Erickson HK, Leece BA, Reid EE, Goldmacher VS, Lambert JM, et al. Synthesis and biological evaluation of antibody conjugates of phosphate prodrugs of cytotoxic DNA alkylators for the targeted treatment of cancer. J Med Chem 2012;55:766–82.
31. Owonikoko TK, Hussain A, Stadler WM, Smith DC, Kluger H, Molina AM, et al. First-in-human multicenter phase I study of BMS-936561 (MDX-1203), an antibody-drug conjugate targeting CD70. Cancer Chemother Pharmacol 2016;77:155–62.
32. van der Lee MM, Groothuis PG, Ubink R, van der Vleuten MA, van Achterberg TA, Loosveld EM, et al. The preclinical profile of the duocarmycin-based HER2-targeting ADC SYD985 predicts for clinical benefit in low HER2-expressing breast cancers. Mol Cancer Ther 2015;14:692–703.
33. Freireich EJ, Gehan EA, Rall DP, Schmidt LH, Skipper HE. Quantitative comparison of toxicity of anticancer agents in mouse, rat, hamster, dog, monkey, and man. Cancer Chemother Rep 1966;50:219–44.
34. Kellogg BA, Garrett L, Kovtun Y, Lai KC, Leece B, Miller M, et al. Disulfide-linked antibody-maytansinoid conjugates: optimization of in vivo activity by varying the steric hindrance at carbon atoms adjacent to the disulfide linkage. Bioconjug Chem 2011;22:717–27.
35. Doronina SO, Mendelsohn BA, Bovee TD, Cerveny CG, Alley SC, Meyer DL, et al. Enhanced activity of monomethylauristatin F through monoclonal antibody delivery: effects of linker technology on efficacy and toxicity. Bioconjug Chem 2006;17:114–24.